Fully frustrated Ising system on a 3D simple cubic lattice: revisited



1999 J. Phys. A: Math. Gen. 32 1787

(http://iopscience.iop.org/0305-4470/32/10/001)

J. Phys. A: Math. Gen. **32** (1999) 1787–1800. Printed in the UK PII: S0305-4470(99)98406-8

# Fully frustrated Ising system on a 3D simple cubic lattice: revisited

L W Bernardi, K Hukushima and H Takayama

Institute for Solid State Physics, University of Tokyo, Roppongi, 7-22-1 Minato-ku, Tokyo 106-8660, Japan

Received 13 October 1998

**Abstract.** Using extensive Monte Carlo simulations, we clarify the critical behaviour of the 3D simple cubic Ising fully frustrated system. We find two transition temperatures and two long-range ordered phases. Within the present numerical accuracy, the transition at higher temperature is found to be second order and we have extracted the standard critical exponents using the finite-size scaling method. On the other hand, the transition at lower temperature is found to be first order. It is argued that entropy plays a major role on determining the low-temperature state.

## 1. Introduction

Nowadays, one of the trends in statistical physics is the study of disorder. The spin glass (SG) problem is the most typical subject in the field which, despite huge theoretical and experimental works, has not yet been solved. Besides disorder, SG also involves frustration which is known to give rise to peculiar, non-trivial, behaviours, especially in Ising systems. Therefore, it is considered as a promising approach to first understand fully frustrated (FF) systems without disorder and then to move closer the SG problem by adding disorder [1]. From this point of view Bernardi and Campbell investigated the critical behaviour along the line from the 3D FF Ising model to the $\pm J$ Ising SG model [2]. In order to gain further insight along this line, we have re-investigated the 3D FF Ising system on a simple cubic lattice which was studied more than a decade ago [1, 3–7] but has been left without thorough understanding. The purpose of this paper is to report our new numerical results on the nature of the phase transitions in this model.

Chui *et al* [3] were the first to point out, by means of the Bethe Peierls approach, that the system exhibits a first-order phase transition at a finite temperature. They also estimated the degeneracy of ground states which grows proportionally to $2^{L^2/4}$ with $L$ being the linear dimension of the system. Blanckschtein *et al* [4] (hereafter referred to as BMB) developed a renormalization group (RG) analysis ($\epsilon$-expansion) based on the Landau–Ginzburg–Wilson (LGW) Hamiltonian which describes critical behaviour of the system of interest. Their main result is that the transition is a weakly first-order one. They also explicitly obtained the 16-fold degenerated ordered configurations of site magnetization just below the transition temperature. Grest [5] attempted to prove BMB's results numerically but the result was inconclusive since the signature of a first-order transition, i.e., a bimodal distribution in the energy histogram, was not seen.

The first numerical study was done by Kirkpatrick [1] which showed that this system exhibits a second-order phase transition at $T_c = 1.25J$ while geometrical argument leads to

0305-4470/99/101787+14$19.50  

the absence of a phase transition. Diep *et al* [6] (hereafter referred to as DLN) carried out the most extensive numerical study on this system and obtained the following results. The transition from the paramagnetic phase to an ordered phase occurs at $T_c = 1.355J$ for the infinite-size limit and is of second order. At lower temperatures the system moves to another phase, in which disorder is located along unidirectional lines which in turn form a periodic array. DLN also mentioned the existence of a crossover behaviour at a temperature higher than $T_c$. Narita et al [7] studied the system by looking at configurations of wrong (or unsatisfied) bonds, and suggested the occurrence of a Kosterlitz–Thouless-like transition and also noted the existence of two and possibly three transitions.

In this paper, by making combined use of the standard Monte Carlo (MC) method and the exchange MC method [8], the nature of the critical behavior in the 3D FF Ising system is clarified. There exists two ordered phases both with long-range ordered magnetization patterns. The pattern in the higher temperature phase below the transition temperature $T_{c1}$ is one of the 16-fold degenerated states predicted by the BMB theory, while the one in the lower temperature phase below the transition temperature $T_{c2}$ is one of the 24-fold degenerated states found by DLN at the lowest temperatures. A mechanism to derive this lower temperature phase, which we call the '$4J$-excitation', is proposed. Within the present numerical accuracy, the transition at $T_{c1}$ ($T_{c2}$) is of second (first) order. The crossover found by DLN above $T_{c1}$ tends to vanish for larger systems.

This paper is organized as follows. In the next section, we will present the model and the methods we have used. Geometrical considerations about the ground states and the $4J$-excitation are given in section 3. In section 4 the simulated results for various quantities, in the whole temperature range, are presented, and in section 5 the nature of the two ordered phases and the associated transitions are discussed in some detail. The last section is devoted to the concluding remarks.

## 2. Model and methods

The model studied is described by the standard Hamiltonian,

$$H = -\sum_{\langle i,j \rangle} J_{ij} S_i S_j \tag{1}$$

where $S_i$ are Ising spins and $J_{ij}$ are nearest-neighbour interactions which take value +1 or $-1$ following patterns described in figure 1(*a*). We call it the DLN model†. Although its bond pattern is different from the one of figure 1(*b*) (BMB model), the critical behaviour of the two models is expected to be the same because every plaquette is frustrated in both systems and, in fact, one can go from one system to the other by gauge transformation. However, in the present simulation we have examined only the DLN model.

In order to investigate critical properties of the model, we have used two MC techniques both making use of the heat-bath updating. One is the standard MC method which has been used to obtain time evolution, including gradual cooling or heating processes, of quantities of interest. The other is the exchange MC method [8]. The basic idea of this method is to simultaneously run several replicas having a common bond configuration but attached to heat baths of different temperatures, and to stochastically exchange a pair of them according to the detailed balance condition for the combined system of all the replicas. The exchange MC (EMC) method is quite efficient at examining equilibrium properties of such a system with many degenerate states.

† Although the first study was done by Kirkpatrick, we will rely on the paper by Diep *et al* and hence the name DLN.

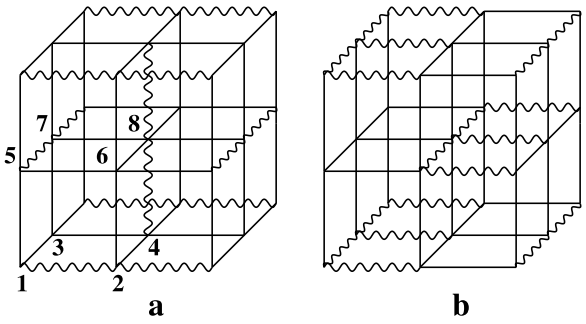


**Figure 1.** The structure of the FF 3D SC (*a*) DLN and (*b*) comb-type (BMB) model. The (wavy) thin line represents the (anti-)ferromagnetic bond. The numbers label the sub-lattices used during the simulation.

In this paper the following quantities are evaluated for systems with $N = L^3$ spins under the periodic boundary condition.

(a) Total internal energy, $E$, and specific heat $C_v$.
(b) Overlap distribution defined by

$$P(q) = \sum_{t=1}^{N_{\mathrm{mcs}}} \delta\left(q - \frac{1}{N}\sum_{i=1}^{N} S_i^a(t) S_i^b(t)\right) \tag{2}$$

where $N_{\mathrm{mcs}}$ is the number of MC steps, and $a$, $b$ label two different replicas.
(c) Sub-lattice energy, $\epsilon_\alpha$, defined by

$$\epsilon_\alpha = \frac{8}{N}\sum_{i\in\alpha}\frac{1}{N_{\mathrm{mcs}}}\sum_{t=1}^{N_{\mathrm{mcs}}}\sum_{j}^{\mathrm{n.n.}} -J_{ij}S_i(t)S_j(t) \tag{3}$$

where $\alpha$ indicates the sub-lattices ($\alpha = 1, \ldots, 8$) which are defined by the eight corners of one of the unit cubes (see figure 1(*a*)).
(d) Site magnetization defined by

$$M_i^s = \frac{1}{N_{\mathrm{mcs}}}\sum_{t=1}^{N_{\mathrm{mcs}}} S_i(t). \tag{4}$$

## 3. Ground states and 4$J$-excitation

A ground state of the Ising system described by equation (1) is a spin configuration having the minimum number of wrong (or unsatisfied) bonds which are defined as $-J_{ij}S_iS_j = +J$. Since all plaquettes in the present 3D FF model are frustrated, a ground state is obtained when all the plaquettes have the minimum number of wrong bonds which is unity. For a ground state of the unit cube, it is easy to see that only three wrong bonds are required, thereby none of them are on a common plaquette and there are two corners which are not touched by them. Actually, there are eight (multiplied by two when global inversion of spin is taken into account) ways of minimizing the energy of the unit cube as shown in figure 2. The generic way to create a ground state of the total system, is to pile up these cubes with the only constraint being that the wrong bond is at the same place for each common plaquette. For example, the neighbour of $a$ in the $x$-direction can be either $c$ or $g$. Let us introduce what we will call *periodic* ground states. If one takes the $c$ cube as a neighbour of $a$, the wrong bond oriented in the $x$-direction

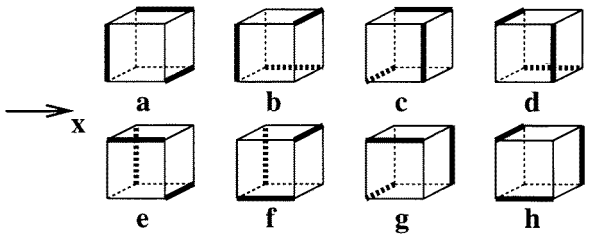


**Figure 2.** The eight ways of minimizing the energy of the unit cube with three wrong bonds (represented by the bold lines).

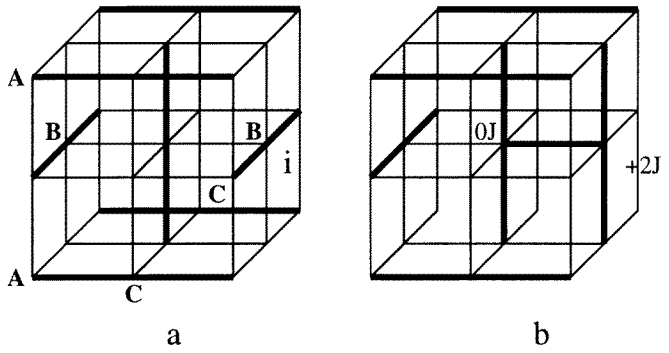


**Figure 3.** All the spins of the line AA, BB or CC can be inverted without changing the total energy.

is continuous (in the $g$ case it is not) and the next neighbour of $c$ in the $x$-direction can be $a$. So the pattern can be $acac\ldots$. In this case the position of the wrong bond perpendicular to the common plaquette has been taken into account. There are only 16 *periodic* ground states since once the first cube is set there is no choice for the neighbouring cube (which gives a degeneracy of $8 \times 2$ for the spin reversal symmetry). In these periodic ground states only two kinds of sites exist when one looks at the sub-lattice energy $\epsilon_\alpha$; $\frac{6}{8}$ sites with $\epsilon_\alpha^{(H)} = -2J$ and $\frac{2}{8}$ sites with $\epsilon_\beta^{(L)} = -6J$.

As first pointed out by Kirkpatrick [1], in each of the periodic ground states, there are lines of spins that can be inverted without changing the total energy of the system. They are the lines AA, BB, and CC in figure 3($a$) and were called bilinear-chain excitations by DLN. Two wrong bonds are connected to each site of these lines. The choice of the lines inverted is restricted to be in the same direction. For example if one inverts the AA line, one site on the adjacent CC line has only one wrong bond and thus inversion of this spin (or this CC line) costs excess energy. Therefore, one needs to count how many lines can be inverted once the direction is chosen. That number is simply given by $L^2/4$ and so degeneracy of the ground states is $2^{L^2/4}$, which is the same order of magnitude as Chui *et al* [3] found. One of the consequence of this inversion is that the neighbouring sites of this line which had energy $-2J$ and $-6J$ before the inversion now have $-4J$.

A further interesting fact is that there is an actual process to invert all spins on one line which costs an energy of only $4J$. In fact, if one spin is flipped, for example, the site $i$ on the BB line in figure 3($a$), the wrong-bond pattern changes to the one shown in figure 3($b$), which has $4J$ higher energy before the flip. But now the internal field at the two neighbouring sites vanishes so that spins on the sites can flip without cost of energy. This mechanism was called

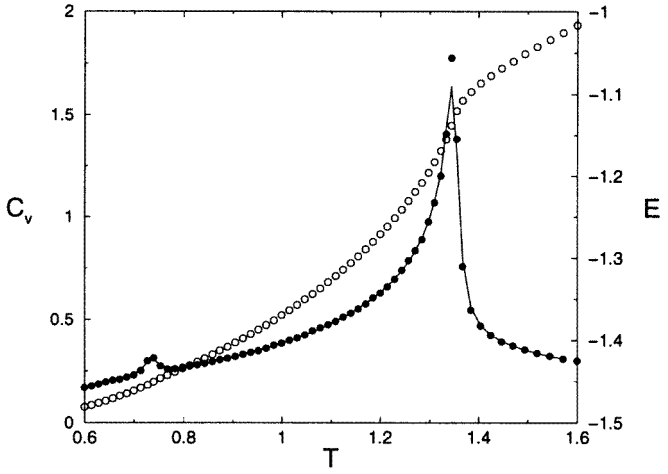


**Figure 4.** The (•) represent the results of the fluctuation of the energy while the solid curve represents the derivative of the energy. The (○) represent the energy. The data were obtained using the EMC method with a system size $L = 24$.

a kink–anti-kink pair by Kirkpatrick [1] but here we call it a $4J$-excitation. With the aid of one $4J$-excitation all spins on the BB line can be inverted. Strictly speaking, this holds under the periodic boundary condition we have adopted. It is important to notice that the presence of one $4J$-excitation is associated with an entropy of $L\ln 2$ which is much larger than its energy $4J$. This indicates, as will be demonstrated below, that entropy plays an important role on determining an ordered phase, if any, at lowest temperatures.

## 4. Results

In this section we present the data in the whole temperature range simulated. They strongly suggest the existence of two phase transitions in the present FF model. Details of their critical nature will be discussed in the next section.

### *4.1. Specific heat and energy*

The results of the specific heat and the energy simulated by the exchange MC method are shown in figure 4. They indicate a second-order phase transition at the temperature $T_{c1}(\simeq 1.35J)$ and the existence of another transition at $T_{c2}(\simeq 0.70J)$.

### *4.2. Overlap distribution*

The overlap distribution $P(q)$ simulated by the exchange MC method is shown in figure 5. It exhibits quite different shapes either from the one of a simple ferromagnet (with only double peaks at $q = \pm m^2$, $m$ being the uniform magnetization) or from the one of the mean-field SG model (with double peaks at $q = \pm q_{\mathrm{EA}}$, $q_{\mathrm{EA}}$ being the Edwards–Anderson order parameter, and continuous weight between the peaks). The characteristic features of $P(q)$ of the present FF model are as follows.

(i) It has a single peak centred at $q = 0$ in the paramagnetic phase ($T > T_{c1}$).

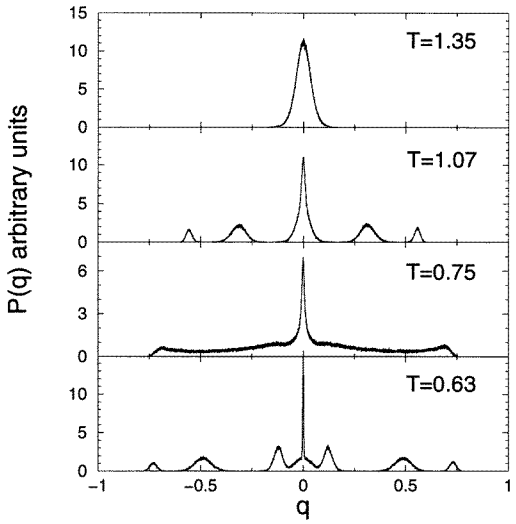


**Figure 5.** Overlap distribution for the FF system. Data obtained with the MCE method with a system of size $L = 32$.

(ii) At $T_{c1} > T > T_{c2}$, five peaks appear. The peaks are narrowed when the size of the system increases. This indicates that there exist several states which are thermodynamically stable. We call the phase of this temperature range the *high-T phase*.

(iii) At $T = 0.75 \simeq T_{c2}$, $P(q)$ exhibits a peak at $q = 0$ with a continuous distribution in both sides of the peak. This implies a certain disordered configuration.

(iv) Below $T_{c2}$ a seven-peak structure appears, indicating the occurrence of another ordered state. We call the phase of this temperature range the *low-T phase*.

### *4.3. Sub-lattice and site quantities*

We have performed standard MC simulations of gradual cooling or heating processes and have looked at evolution of the sub-lattice energy $\epsilon_\alpha$. The results are shown in figure 6. The lines represent evolution with temperature of the eight $\epsilon_\alpha$. For each point $10^4$ MCS of annealing were used and the next $10^4$ MCS were used to get $\epsilon_\alpha$. Each curve in the figure represents the result of a single MC run but we have checked that other runs qualitatively give the same results.

From figure 6.*a* we can extract the following characteristic features of the gradually cooling process. First of all the sub-lattices are linked two by two. In the high-$T$ phase ($T_{c1} > T > T_{c2}$) there exist two kinds of sub-lattices. The one with lower energy, $\epsilon_\alpha^{(L)}$, consists of two sub-lattices which are directly checked to be located at opposite corners of the cube. The other with higher energies, $\epsilon_\alpha^{(H)}$, consists of the other six sub-lattices. As the system is cooled gradually $\epsilon_\alpha^{(L)}$ decrease, while $\epsilon_\alpha^{(H)}$ stay nearly constant ($\simeq -2J$). In this phase the system thus exhibits a symmetry similar to the one of the periodic ground state mentioned previously. In the low-$T$ phase ($T_{c2} > T$) there seem to exist three kinds of sub-lattices. Four sub-lattices have $\epsilon_\alpha$ of $-2J$. The other four sub-lattices are grouped two by two with two different $\epsilon_\alpha$ which are symmetric around $-4J$. This symmetry has already been discussed in the discussion of the periodic ground state when the inversion of lines of spin is introduced. But this symmetry does not hold for case 6.*b*, where the system was heated from the ferromagnetic ground state,

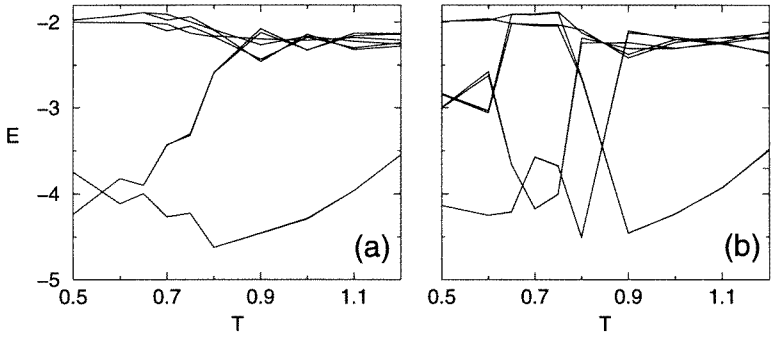


**Figure 6.** Typical sub-lattice energy. (*a*) is obtained by slow cooling while (*b*) is obtained during the heating of a ferromagnetic spin configuration from $T = 0.50$. All the data points were obtained during the same run for a system of size $L = 24$.

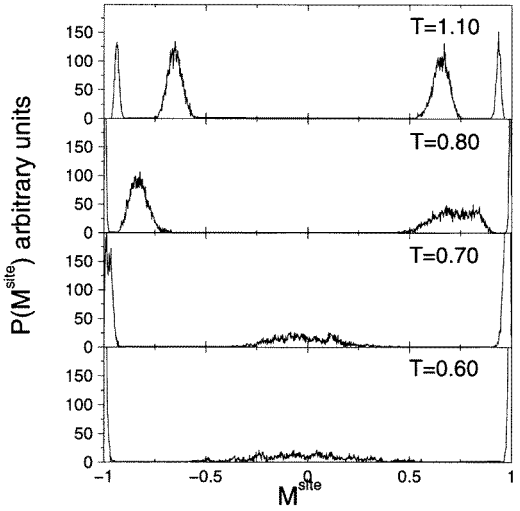


**Figure 7.** Histogram of the site magnetization. Note that for $T = 0.80$, 0.70 and 0.60 there is a peak in $M^{site}$=1 which has been truncated for clarity purposes. In this case the system is of size $L = 24$.

because the annealing time was not long enough at this low temperature. It, however, implies that the ferromagnetic configuration is not stable at finite temperatures.

By the same cooling procedure as described above, we have examined site magnetization, $\{M_i^s\}$. Its distributions in magnitude at four typical temperatures are shown in figure 7. At $T = 1.10$, in the high-$T$ phase, there are four peaks. However, here we discuss about distributions against absolute magnitude of $\{M_i^s\}$, since their signs depend on configurations simulated, similarly to those of the 16 periodic ground states. In this sense there are two kinds of $\{M_i^s\}$, one with smaller $|M_i|$ and the other with the larger one. The integration of the peaks centred around $|m_1|$ and $|m_2|$ yields $\frac{6}{8}$ and $\frac{2}{8}$, respectively. Actually, when the corresponding spatial pattern of $\{M_i^s\}$ is visualized, it is almost perfectly periodic, and agrees with the one derived by the BMB (see section 5.1). When temperature approaches $T_{c2}$ the position of the two peaks tend to saturate to the limiting value, i.e., unity.

At $T = 0.70J$ and $0.60J$, in the low-$T$ phase, there is a flat bump around zero. The

integration of this bump yields a weight of $\frac{2}{8}$, while the two sharp peaks at $\pm 1$ have weight of $\frac{6}{8}$. In the corresponding spatial patterns of $\{M_i^s\}$ we have observed that lines with nearly zero magnetization form a periodic lattice, as found by DLN. This configuration is attributed to the $4J$-excitation mentioned previously (see section 5.3).

## 5. Discussions

The results of our MC simulations presented in the previous section reveal that there exist two ordered phases in the DLN model. In the following we discuss the nature of the two phase transitions in detail.

### *5.1. High-T phase*

When the system is cooled from the paramagnetic phase, an ordered phase appears at $T = T_{c1} \simeq 1.35J$ (see figure 4), which we have called the high-$T$ phase. It is in good agreement with the one theoretically predicted by BMB, which can easily be gauge-transformed from their comb-type model to the one used by DLN.

In the DLN model the magnetic unit cell consists of eight unit cubes as shown in figure 1. In the BMB model, on the other hand, it consists of 16 cubes. There exist 16 degenerated equilibrium configurations including the spin up–down symmetry. Each elementary cube has $|M_i^s| \sim m$ at two diagonally opposite sites, and $|M_i^s| \sim m/a$ with $a > 1$ at other sites with signs specified in such a way that three wrong bonds do not intersect and that they do not touch the two sites with larger $|M_i^s|$. We note that these configurations are different from the periodic ground states for which $a = 1$, and that they minimize the LGW Hamiltonian of the present FF system [4].

The ordered configurations mentioned above are quite consistent with our simulated data described in the previous section. Concerned with the overlap distribution $P(q)$ at $T = 1.07$ shown in figure 5, the positions and weights of the five peaks are what are expected if the system visits the 16 degenerated configurations with equal probability in the exchange MC simulation. The occurrence of these ordered states is also confirmed by the $\{M_i^s\}$-histogram at $T = 1.10$ shown in figure 7, and by the direct inspection on the spatial pattern of $\{M_i^s\}$ (not shown). Furthermore, in figure 8 we plot $R$, the ratio of positions of the two peaks in figure 7 against temperature. The results are consistent with the theoretical prediction $a = \sqrt{3}$ [4] expected to hold at a temperature close to $T_{c1}$.

In contrast to the previous arguments by Narita et al [7] and DLN, our simulated data strongly suggest that each of the 16 degenerated configurations is long-range ordered (or thermodynamically stable). To confirm this we have computed the sub-lattice switching time, $\tau_{sc}$. By inspection of time evolution of each sub-lattice energy $\epsilon_\alpha$ at a fixed temperature close to $T_{c1}$ we have observed that it fluctuates between the higher and lower branches of $\epsilon_\alpha$ in figure 6 with an average interval of $\tau_{sc}$ which grows with the size of the system. To extract $\tau_{sc}$ more accurately we have used the autocorrelation function $q(t)$ which almost saturates to an equilibrium value before exhibiting an exponential decay. This exponential decay, at the later stage, is attributed to the sub-lattice switching and its relaxation time is examined at $T = 1.32(<T_{c1})$ for $L$ sizes varying from 12–28. The result shown in figure 9 indicates that $\tau_{sc}$ is exponential with an argument growing roughly linearly with $L$. This implies that in this 3D FF model the domain-wall free-energy is roughly proportional to $L$ (and not to $L^2$ as for an ordinary 3D ferromagnet), and that the sub-lattice switching does not occur in the thermodynamic limit.

The technique usually used to know the domain-wall free-energy, is the defect-free-energy

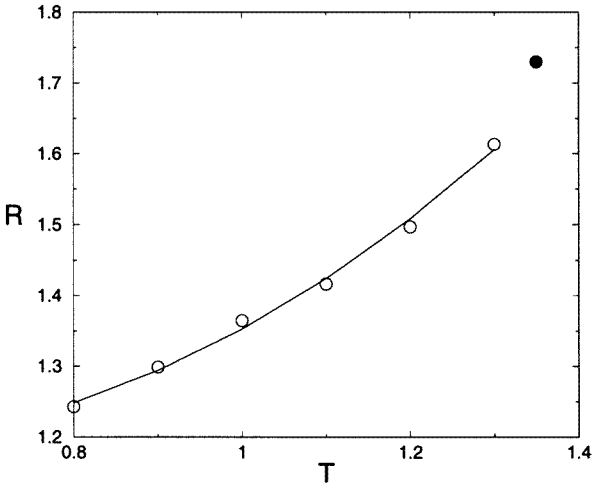


**Figure 8.** The ratio, $R$, of the larger to the smaller site magnetization against temperature. The (•) represent the theoretical value of $R$ at $T_{c1}$. The curve is a guide to the eye.

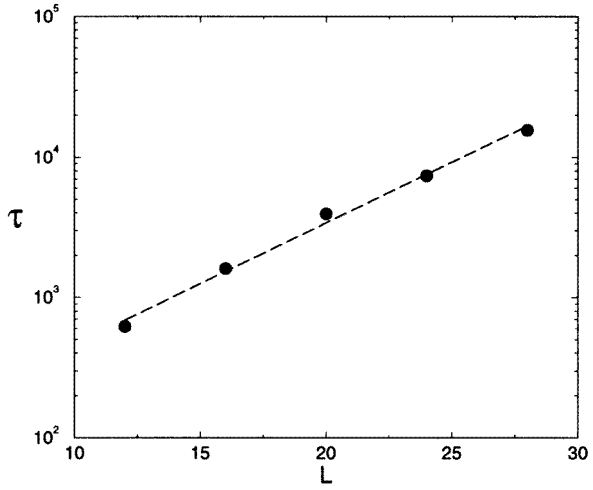


**Figure 9.** Time of sub-lattice switching, $\tau$ against the size of the system, $L$. Note the linear-log plot.

analysis [9]. The principle is to introduce a domain-wall in a system and to see how the energy is affected by this domain. If the energy increases with the size then the system exhibits a phase transition. To obtain the domain wall free-energy one computes

$$\Delta F = F_{AP} - F_P \tag{5}$$

where $F_{AP}$ and $F_P$ are the free-energy of the system for the anti-periodic (AP) boundary and periodic (P) boundary conditions, respectively. With standard MC simulations the free-energy can be obtained by

$$\beta F(T) = \int_{\beta_{min}}^{\beta} \mathrm{d}\beta' \, E(\beta'). \tag{6}$$

In the simulation the $\beta_{min}$ is set to $(10J)^{-1}$ and we assume that $\Delta F$ is negligible at $\beta_{min}$. The

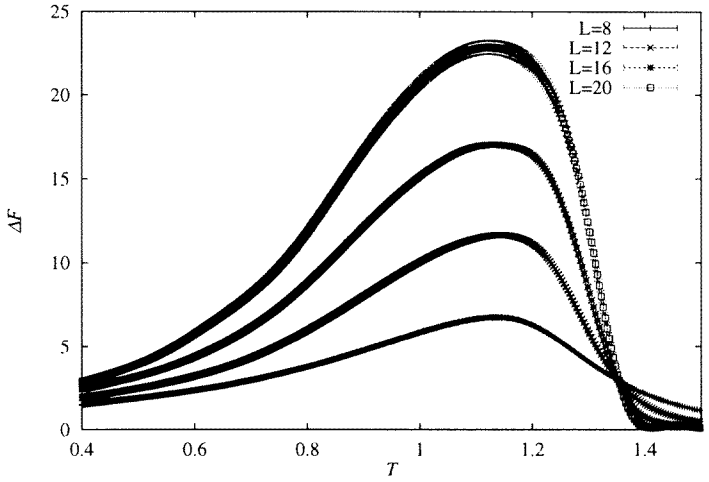


**Figure 10.** Results for the defect-free-energy analysis for sizes $L = 8$, 12, 16 and 20.

results are shown in figure 10 where we can see that the maximums of $\Delta F$ also have a nearly linear dependence in $L$. We can also note that the two low temperature phases have a different slopes for $\Delta F$ against $T$.

### *5.2. Critical nature of the transition at $T_{c1}$*

According to BMB, the LGW Hamiltonian for describing the phase transition in the present FF model is an $n = 4$ 'Heisenberg' model with symmetry breaking terms arising from frustration. The RG analysis based on the $\epsilon$-expansion method predicts a weakly first-order phase transition. Within our present numerical accuracy, however, we have not detected any evidence which supports a first-order transition at $T_{c1}$ (see, for example, figure 4 and further discussions in section 6). The present results are in agreement with the previous numerical works by DLN and Grest [5].

Assuming a second-order transition at $T_{c1} = 1.347 \pm 0.001$, we have obtained the following critical exponents:

$$\alpha = 0.32 \pm 0.02 \qquad \nu = 0.56 \pm 0.02 \qquad \beta = 0.25 \pm 0.02 \qquad \eta = -0.1 \pm 0.02. \quad (7)$$

These exponents are different from those of the O(4) model and we do not know to which class of universality they belong. The exponent $\alpha$ of specific heat is estimated either directly as shown in figure 11, or by the finite-size scaling shown in figure 12. In relation to our results demonstrated in figure 11, it is noted that the apparent crossover within the paramagnetic phase observed by DLN is considered to be an artifact due to finite-size effect. Correspondingly, our exponents $\alpha$ and $\nu$ are compatible with those obtained by DLN at temperatures above the crossover whose data are not considered to be affected by the finite-size effect. The $\eta$ value given by DLN ($\simeq$0.28) being obtained at $T_{c1}$ is considered to be affected by finite-size effect.

The Binder cumulant [10] method is frequently used to determine the exponents $\nu$ and $\beta$. From the latter the exponent $\eta$ is calculated by the scaling relation $\frac{2\beta}{\nu} = d - 2 + \eta$. However, for the present FF model with the degenerated ordered states below $T_{c1}$ and with the presence of the peak at $q = 0$ in $P(q)$, a direct application of the method is rather complicated. This problem for the Binder cumulant had already been pointed out for the three states Potts models [11].

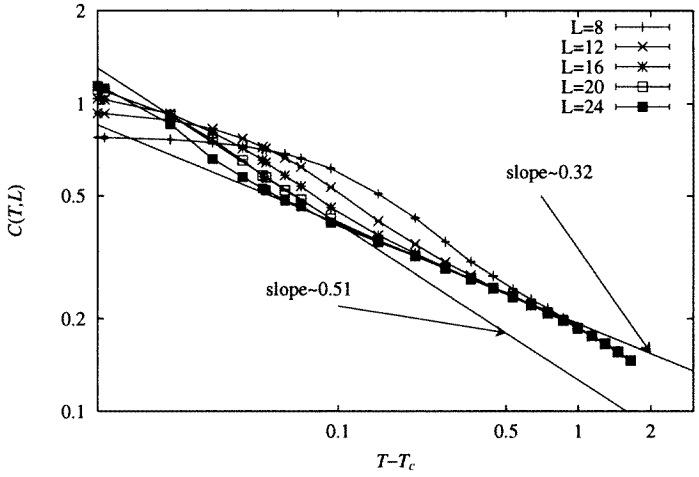


**Figure 11.** Size dependence of the specific heat near $T_{c1}$.

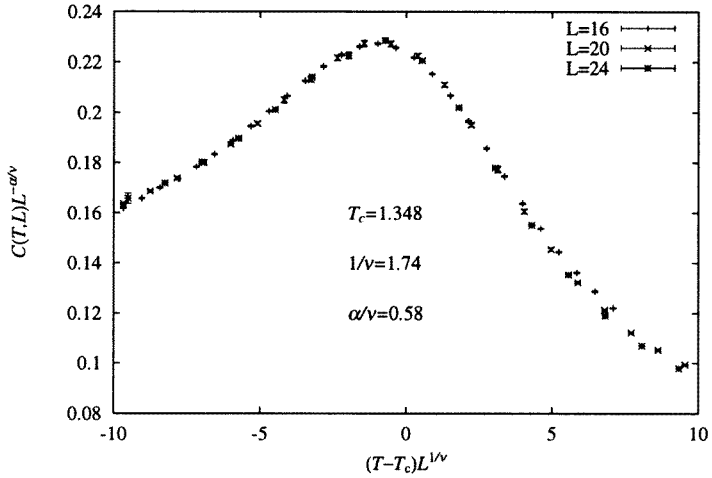


**Figure 12.** Scaling plot of the specific heat.

Instead we have analysed the finite-size scaling of the following ratio [12]:

$$R_2(L_1, L_2) \equiv \log\left(\frac{\langle q^2_{L_2}\rangle}{\langle q^2_{L_1}\rangle}\right) \Big/ \log\left(\frac{L_2}{L_1}\right) = -2\frac{2\beta}{\nu} + g(L_2^{1/\nu}(T - T_c)) \qquad (8)$$

with $g(x)$ being a scaling function and $L_2 > L_1 \gg L_2 - L_1$. The factor 2 in the r.h.s. of the above equation came out because $\langle q^2\rangle$ is given by the following scaling form:

$$\langle q^2\rangle = \left\langle \left(\frac{1}{N}\sum_i^N S_i^\alpha S_i^\beta\right)^2 \right\rangle_T = \frac{1}{N^2}\sum_{i,j}^N \langle S_i^\alpha S_j^\alpha S_i^\beta S_j^\beta\rangle_T \qquad (9)$$

$$= \frac{1}{N^2}\sum_i^N G_{ij}^2 \propto L^{-2(d-2+\eta)} f(L^{\frac{1}{\nu}}(T - T_c)) \qquad (10)$$

where $\langle\cdot\cdot\rangle_T$ is the thermal average and $f(x)$ another scaling function. Here $G_{ij}$ is the correlation

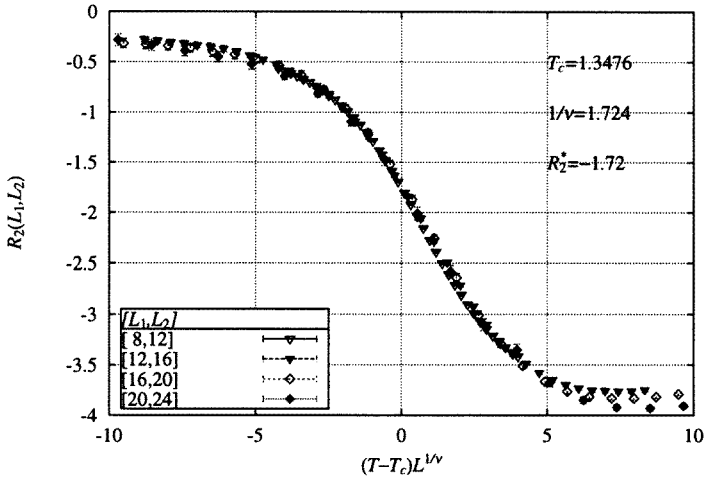


**Figure 13.** Scaling plot of $R_2(L_1, L_2)$.

function $\langle S_i S_j \rangle_T$ which is given by

$$G_{ij} = G(r = |x_i - x_j|) \propto r^{-(d-2+\eta)} \exp\left(\frac{-r}{\xi}\right). \tag{11}$$

Thus the crossing point of $R_2(L_1, L_2)$ with different set of $(L_1, L_2)$ will be $(T_c, -\frac{4\beta}{\nu})$. The scaling plot of $R_2(L_1, L_2)$ giving $T_{c1}$, $\nu$ and $\beta$ is shown in figure 13.

### *5.3. Low-T phase and nature of the transition at $T = T_{c2}$*

As temperature decreases in the high-$T$ phase, the larger $|M_i^s|$ become almost saturated to unity. Then the arguments based on the LGW Hamiltonian, in which no restriction on the magnitude of $M_i^s$ is imposed, are expected to break down. In fact, as already described in section 4, the transition to the low-$T$ phase occurs around $T = T_{c2} \simeq 0.7$.

In each of spin configurations in the low-$T$ phase realized by the gradual cooling MC process, one fourth of all the chains in one of the three directions are disordered ($|M_i^s| \simeq 0$), while the others have almost saturated value ($|M_i^s| \simeq 1$). Furthermore, these disordered chains form a periodic 2D array. Thus the low-$T$ phase is 24-fold degenerated as pointed out by DLN. This degeneracy is responsible for the positions and weights of the seven-peaks structure in $P(q)$ shown in figure 5. We argue that the above-mentioned order in the low-$T$ phase is attributed to the $4J$-excitation introduced at the end of section 3. As pointed out there, the presence of one $4J$-excitation lowers free-energy by $-TL\ln 2 + 4J$ as compared with the state without it. This holds true so long as the eight chains surrounding the disordered chain (with the $4J$-excitation) are firm and play a role of a *cage* of the latter. Also, we can at least check that two $4J$-excitations on two chains perpendicular to each other cannot cross freely. Therefore for the system to have maximum free-energy gain a periodic array of $L^2/4$ disordered chains is realized.

It is rather hard to check the thermodynamic stability of each of the 24 degenerated states in this phase, not only because MC dynamics become slower at these low temperatures, but also because system sizes have to be large enough for an almost ideal random walk of $4J$-excitations to be realized. Also free-energy barrier between the different states become small as temperature decreases. In fact, as seen in figure 10, magnitudes of defect-free-energy tend

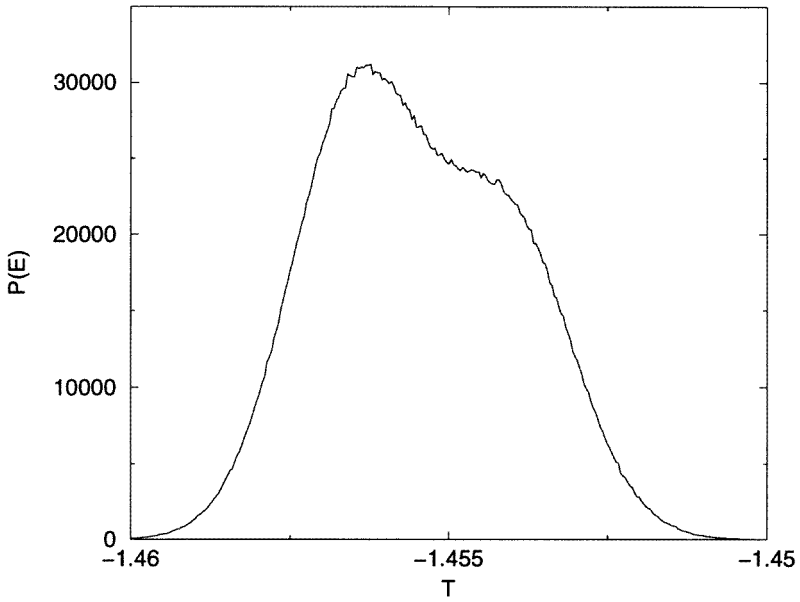


**Figure 14.** Histogram of the energy for $L = 48$ at $T = 0.716$ obtained with $4 \times 10^6$ MCS. The histogram shows a double-peak structure implying a first-order phase transition.

to decrease from around $T_{c2}$ with decreasing temperature. But since those with the larger $L$ still have the larger values, we expect that each of the 24 states are thermodynamically stable. In this context, it is noted that defect-free-energy at $T = 0$, is easily checked to vanish. This, combined with existence of the $4J$-excitation, implies that stability of (or free-energy barriers between) the ordered states so far discussed, is guaranteed solely by the entropy effect.

Finally, we discuss the nature of the transition at $T_{c2}$ between the high-$T$ and low-$T$ phases. The transition is expected to be of first order, since it occurs between spin configurations having different symmetries with 16-fold and 24-fold degeneracy. This can easily be seen from the fact that the ratio of larger to smaller site magnetization shown in figure 8 does not extrapolate to one at $T_{c2}$ for the high-$T$ phase, while it is, by definition, one in the low-$T$ phase for the spin in the *cage*. Among our numerical data, a peculiar shape of $P(q)$ at $T = 0.75$ shown in figure 5, the appearance of a significantly large hysteresis in various quantities, and, most plausibly, the energy histogram with a double-peak structure shown in figure 14 support this argument. The double-peak structure was not seen with size smaller than $L = 48$ and we expect that simulations with larger size will give a better separation between peaks although it is too cpu time consuming at the present time.

## 6. Concluding remarks

We have shown by extensive MC simulations the nature of the phase transitions in the 3D FF Ising model. The driving mechanism of the lower transition at $T_{c2}$ agrees with what DLN proposed, though we have further introduced the '$4J$-excitation' mechanism explicitly. We have also claimed that this transition is of first order. The nature of the high-$T$ phase below $T_{c1}$ is quite consistent with the prediction by the BMB theory. Although our results simulated in this paper strongly suggest a second-order phase transition at $T_{c1}$, we cannot exclude the possibility that it is of first order when studied in systems with larger sizes and at closer

temperatures to $T_c$ as is the case for other systems exhibiting a weak first-order transition [13]. The search for this possibility is now underway.

This paper reveals that the transition behaviours of the present FF model are dominated by a subtle balance of the entropy effects. They are expected to be affected sensitively if disorder is added. In particular, behavior of the $4J$-excitation in the presence of small disorder is of interest. Analysis along this direction is also underway.

*Note added in proof.* The critical exponents of this system are close to the one of the $XY$ stacked triangular antiferromagnetic model given by Kawamura [14]. The reason why these two systems have the same critical exponents is unknown to us.

## Acknowledgments

We would like to thank Professor I A Campbell for valuable discussions. Numerical calculations were mainly performed on the Fujitsu VPP500 at the Super Computer Center in the Institute for Solid State Physics. This work is supported by a Grant-in-Aids for International Scientific Research Programme (no 10044064) and a Grant-in-Aids for Scientific Research Programme (no 10640362) both from the Ministry of Education, Science, Sport and Culture. LWB was supported by a Fellowship of the Japanese Society for Promoting Science.

## References

[1] Kirkpatrick S 1981 *Lecture Notes in Physics* vol 149, ed C Castellani *et al* (Berlin: Springer) p 280
[2] Campbell I A and Bernardi L 1996 *Phys. Rev.* B **52** R9819
[3] Chui S F, Forgacs G and Hatch D M 1982 *Phys. Rev.* B **25** 6952
[4] Blankschtein D, Ma M and Nihat Berker A 1984 *Phys. Rev.* B **30** 1362
[5] Grest G S 1985 *J. Phys. C: Solid State Phys.* **18** 6239
[6] Diep H T, Lallemand P and Nagai O 1985 *J. Phys. C: Solid State Phys.* **18** 1067
[7] Narita Y, Ono I and Oguchi T 1986 *J. Phys. Soc. Japan* **55** 3778
[8] Hukushima K and Nemoto K 1996 *J. Phys. Soc. Japan* **65** 1604
Tesi M C, Janse van REnsburg E J, Orlandini E and Whittington S G 1996 *J. Stat. Phys.* **82** 155
[9] Muller-Hartmann E and Zittartz J 1977 *Z. Phys.* B **27** 261
[10] Binder K 1981 *Phys. Rev. Lett.* **47** 693
[11] Vollmayr K, Reger J D, Sheucher M and Binder K 1993 *Z. Phys.* B **91** 113
[12] Miyashita S, Nishimori H, Kuroda A and Suzuki M 1978 *Prog. Theor. Phys* **60** 1669
[13] Peczak P and Landau D P 1989 *Phys. Rev.* B **39** 11 932
[14] Kawamura H 1998 *J. Phys.: Condens. Matter* **10** 4707